Robust Optimization with Credibility Factor for Graph-based SLAM

Long Chen[1*], Jun Yang[1], Yuhang He[2] and Kai Huang[1]

***Abstract*— Graph-based Simultaneous Localization and Mapping (SLAM) refers to formulate SLAM by a graph model whose nodes represent poses of the robot and whose edges represent constraints relating the poses, then solve an error minimization problem to find the configuration of the poses that best fits with the constraints. One problem of state-of-the-art SLAM algorithms is that they rely on all the poses and constraints with the same credibility and do not fully exploit the different confidence levels of different poses and constraints. This paper proposes a novel formulation that involves the credibility factor of the poses and constraints into the graph model. The proposed optimization model that updates the graphical model with switch variables and credibility factors, which removes wrong loop closures and increases the overall accuracy by keeping the poses with higher credibility factor more stable and the poses with lower credibility factor more elastic. The results of several experiments conducted on large scale synthetic and real datasets are provided to demonstrate the credibility and effectiveness of the method.**

I. INTRODUCTION

Simultaneous Localization and Mapping (SLAM), which solves the problem that how to build a map of an unknown environment or update a map of a known environment and to simultaneously localize itself within the map, has been a core technology in the field of autonomous robotics and intelligent vehicles.

State-of-the-art SLAM structure usually consists of a front-end part and a back-end part. The front-end analyzes the available sensor data, performs data association to detect right loop closures and build factor graph which is used to express the least squares optimization problem for SLAM. The back-end optimizes the factor graph by applying non-linear least squares optimization techniques to obtain a map that describes all the access information perfectly.

Nowadays, optimization-based approaches for full-SLAM problem become more and more popular. This kind of method was first proposed in the robotics community for 2D laser scans by Lu and Milois in 1997 [1] and now its prominent examples have been the so-called pose graphs (see Fig. 1) of Olson [2], TreeMap [3], iSAM [4], iSAM2 [5], g2o [6] and others [7], [8]. These optimization-based approaches for nonlinear optimization fully and deeply discover the sparse feature in the SLAM problem so that large scale SLAM problems containing several 10k poses, edges and loop closures can be solved in several seconds on standard hardware. Recently, Sünderhauf and Protzel [9] present a robust back-end which introduces switch valuables [10] to remove false positive loop closures and still converges towards the correct solution.

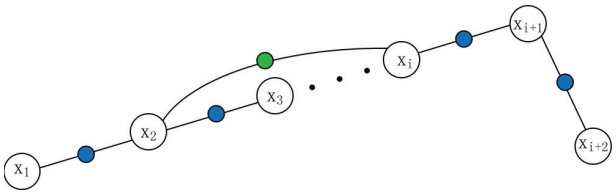

Fig. 1. Factor graph used to describe the pose graph SLAM problem. The unknown poses are represented by large white nodes, whose probabilistic constraints are shown by the small nodes. Odometry constraints between consecutive poses are expressed in blue. The green nodes stand for loop closure between discrete poses.

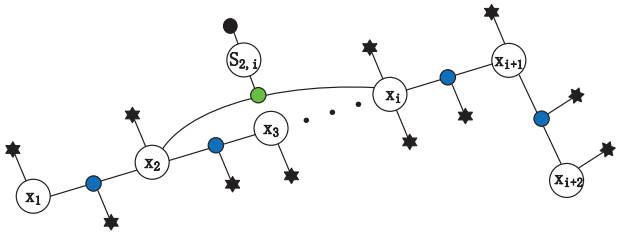

Fig. 2. Factor graph with credibility constraint. Individual robot pose nodes are connected by odometry factors (blue). The switch variable $s_{2,i}$ is used to switch off the false loop closure factor (green). The switch variable is controlled by a prior factor (black) that limits the error probability of loop closure. The black stars attached with poses and odometry factors refers to the credibility value of the related poses and odometry factors.

However, the back-end optimization methods mentioned above overly focus on how to optimize the graph model, but neglect how to make full use of the front-end information which could contribute to update the structure of the graph model and improve the accuracy of maps. For instance, most back-end optimization methods think all the poses and constraints they get from the front-end have the same credibility by default. Actually, the confidence level of different poses and constraints should be different. Analogy to perception of the environment by people, people will treat different places or locations with different confidence degrees based on prior knowledge and common sense. Just like Eiffel Tower is in Paris, U-turn signs always occur in front of an intersection.

In real applications, some scenarios which have information of features deserve to be used for getting the corresponding credibility. Corners, hallways, objects, landmark, etc., are features which can be recognized easily by feature detection or matching algorithm in *front-end* [11]. In the field of surveying and mapping, some special sites are often measured previously as the control points [12] which are regarded as high-precision prior poses to assist localization.

[1]L. Chen, J.Yang and K. Huang are with Sun Yat-sen University, Zhuhai, Guangdong, P.R.China

[2]Y. He is with Wuhan University, Wuhan, Hubei, P.R.China.

*Corresponding Author: Dr. L. Chen, chenl46@mail.sysu.edu.cn.

Obviously, if these prior values are acquired in advance, then a more precise map can be created. Some researchers have utilized the prior information to assist robot localization. Korah and Rasmussen [13] use an image processing technique to extract road information of aerial images. Montemerlo and Thrun [14] provide a method to get prior information from GPS. Rainer Kümmerle's team in 2011 [15] extended the MCL to achieve an online optimization of pose graph by using aerial images as prior information.

Based on the assumption that different poses and constraints should have different credibilities, we propose a novel pose graph structure to model the SLAM problem on the basis of Niko's robust back-end method [16]. The proposed pose graph model introduces credibility factor for each pose and constraint to the back-end graph model, which is shown in Fig. 2. The contributions of this paper are as followed,

1) Credibility factor is introduced into the graph-based SLAM solution. The back-end optimizer can trust the data with higher credibility more and reduce the interference from the data with lower credibility, instead of treating all the data with the same confidence level.
2) The proposed method can update the graph model with switch variables and credibility factors. The Gauss-Newton method and the updated Marquadt's method are combined to remove wrong loop closures and increase the accuracy of maps.
3) Different types of policies to arrange high-credibility prior poses are simulated and a large number of experiments are done to prove the correctness and robustness of our precise back-end. The results show that our method increases the accuracy of maps.

II. CREDIBILITY FACTOR GRAPH SLAM

The proposed graph model relies on a robust graph-based formulation of SLAM problem and Marquardt's Method [17] for the non-linear least squares problem. The pose graph SLAM problem is modeled as a factor graph [18], which is an useful model to express the large global factor problem by small subsets with lots of nodes. In a full SLAM problem, the map M and the robot poses $X = \{x_i\}$ are unknown priori knowledge, which have to be estimated using the information given by the front-end part. The motion constraints $U = \{U_i, U_{ij}\}$ are usually given by front-end. Here, u_i presents the odometry constraints between two consecutive poses x_i and x_{i+1}, u_{ij} refers to the loop closure between two discrete poses x_i and x_j. A nonlinear function f is used to present the motion model of the robot.

$$x_{i+1} = f(x_i, u_i) + w_i \tag{1}$$

The zero-mean Gaussian is often used to model the noise of the odometry system. Where the term w_i follows a Gaussian distribution,

$$w_i \sim N(0, \Sigma_i) \tag{2}$$

Here, Σ_i is the related covariance. And then, x_i can be modelled using a Gaussian distribution as followed,

$$x_i \sim N(f(x_{i-1}, u_{i-1}), \Sigma_i) \tag{3}$$

Besides, x_i can be modelled using another Gaussian distribution with covariance Λ_{ij}, when it is in a loop closure,

$$x_i \sim N(f(x_j, u_{ij}), \Lambda_{ij}) \tag{4}$$

The probability for all the nodes X and constraints $U = \{U_i, U_{ij}\}$ is as followed

$$P(X|U) \propto \prod_i P(x_{i+1}|x_i, u_i) \cdot \prod_{i,j} P(x_j|x_i, u_{ij}) \tag{5}$$

The probability distribution $P(X|U)$ which corresponds to maximum a posteriori configuration of robot poses X^* is the key to solve pose graph SLAM. Here X^* stands for the nodes where the distribution gets the maximum value. With the fact that (3) and (4) hold and thus the conditional probabilities of SLAM are all Gaussian, the optimal variable configuration X^* can be obtained as follows,

$$\begin{aligned} X^* &= \arg\max_x P(X|U) \\ &= \arg\min_x -\log P(X|U) \\ &= \arg\min_x \sum_i \|f(x_i, u_i) - x_{i+1}\|^2_{\sum_i} \\ &+ \sum_{ij} \|f(x_i, u_{ij}) - x_j\|^2_{\bigwedge_{ij}} \\ &+ \sum_{ij} \|(x_i - x_i^0) \cdot \varepsilon_i\|^2_{\sum_i} \end{aligned} \tag{6}$$

In this paper, a variable $\varepsilon_i \in [0, 1]$ refers to the credibility factor of each pose x_i. Where $\varepsilon = 1$ means the pose x_i is with highest-credibility. x_i^0 is the initial value of the prior pose. Actually the pose with higher credibility factor means the pose is with higher precision. Similarly the pose with $\varepsilon = 0$ means the accuracy of the pose is lowest. In this paper, we also refer the pose with high credibility as the high-precision prior pose. All the edges are marked with switch valuables to distinguish outlier using the policy in [10]. The problem formulation is updated as followed:

$$\begin{aligned} X^*, S^* = \arg\min_{X,S} & \sum_i \|f(x_i, u_i) - x_{i+1}\|^2_{\sum_i} \\ &+ \sum_{ij} \|\Psi(s_{ij})(f(x_i, u_{ij}) - x_j)\|^2_{\bigwedge_{ij}} \\ &+ \sum_{ij} \|(x_i - x_i^0) \cdot \varepsilon_i\|^2_{\sum_i} \\ &+ \sum_{ij} \|\gamma_{ij} - s_{ij}\|^2_{\Xi_{ij}} \end{aligned} \tag{7}$$

Here, $\Psi(s_{ij})$ means the switch valuable on loop closure u_{ij}, γ_{ij} contains the initial value of switch valuable, Ξ_{ij} is the switch prior variance.

In order to get a relative fast and robust result, the combination of Gauss-Newton and Marquardt's algorithm is introduced in this paper. Essentially, formulation (7) can be presented as

$$X^* = \arg\min_x F(X) \tag{8}$$

Where

$$F(X) = \frac{1}{2}\sum_{i=1}^{m}(f_i(x))^2 = \frac{1}{2}\|f(x)\|^2 = \frac{1}{2}f(x)^T f(x) \tag{9}$$

In Marquardt's method [17], we get the initial estimate X_0 which must satisfy the condition that

$$F^{'}(X_0) = 0 \tag{10}$$

Here, X_0 is a n-dimentional matrix. Obviously, this method treats the poses equally. However, their accuracy is different. So a step is added to update the X_0 properly:

$$X_0 = W \cdot (X_0 - x) + x \tag{11}$$

In this step, the poses with high credibility are fixed subtly without breaking the optimization of low-credibility poses. Provided that f has continuous second partial derivatives, its Taylor series can be written as

$$f(x+h) = f(x) + \jmath_f(x)h + O(\|h\|^2) \tag{12}$$

Then, the step h_M is computed by the following definition

$$(j_f^T J_f + \mu I)h_M = -g \quad with \quad g = j_f^T f(x) \quad and \quad \mu \geq 0 \tag{13}$$

Here, J_f is the Jacobian matrix of f(x), μ is a art damping parameter to control the step size. At each iteration the error of the new configuration is monitored. If the new error is lower than the previous one, μ is decreased for the next iteration. Otherwise, the μ is increased. More detailed description of μ refers to the Marquardt's Method [17]. Usually, this step can increase the accuracy of low-credibility poses, but reduce the accuracy of high-credibility poses at the same time because the pose deviates from the initial pose which is with high precision. Then, this step is optimized by the following formulation

$$X_{k+1} = X_k + W \cdot h_M \tag{14}$$

Finally, the last two steps are calculated cyclically until the system comes to final convergence.

In fact, we equate those high-credibility poses and other poses at each iteration step so that they can influence each other. The work we do additionally is that we keep the position of high credibility poses fixed after each iteration by the formulation (13) and (14). As a result, the high-credibility poses can be protected and drag those low-credibility poses closer to the ground truth at each iteration. The Precise and Robust Back-End Algorithm for SLAM can thereby close the wrong loop closures, protect those high-credibility poses and optimize those low-credibility poses at the same time.

III. THE EXPERIMENTAL DATASETS

To prove the robustness of the proposed approach and show its correctness and generality, this paper uses four synthetic datasets including Manhattan [2], City1000 [4], Ring and RingCity [10] and three real datasets including Rawseeds [19] and Bovisa that have been used in lots of related work in the literature. All experiments were conducted on an Intel Core i3 CPU. The precise and robust back-end formulation was implemented on the basis of the frameworks g2o [6] and vertigo [20].

A. The high-credibility prior poses

All the synthetic and real-world published datasets do not contain the credibility factors for poses or constraints originally. We introduce some possible method to obtain the credibility factors.

The Rawseeds project [19] proposes some techniques for indoor/outdoor ground truth collection. In indoor environment, ground truth has been collected by the use of multi sensors. Besides, the ground truth collected only cover a subset of full robot path. All the robot trajectories have been designed carefully to make sure that multiple loops are closed in ground truth area. A standard RTK-GPS with precision up to 2-6 centimeters is used to collect ground truth in outdoor environments, and a proper collection time which can influence the reception of GPS satellite signals is chosen to get a more accurate ground truth.

All the ground truths of these synthetic datasets used in the paper are provided by cite papers. The high-credibility poses in this paper are all from these synthetic/real ground truth, and are added to those test datasets at related position using place recognition method based on bag of words [21].

These techniques for ground truth collection are rather complex. However, with our method, a more accurate map can be obtained as long as several high-credibility poses on the vehicle path are collected in advance. The main benefit of our method in real world is as follows. When a wide range environment need to be measured, the standard RTK-GPS and camera can be used to collect several points with their coordinates and related environments as high credibility poses firstly. And then, normal collection can be done. Finally, the back-end optimization can be done with our algorithm to get a better result. For example, when the vehicle drives through a mixture indoor/outdoor environment, a better map can be obtained with adding several high-credibility poses which are provided by a standard RTK-GPS(see Fig. 4(b),Fig. 4(c)).

IV. EVALUATION METHOD

To valuate feasibility of our graph model, the credibility factors are artificially inserted to the datasets in a simplified way. Most poses are assigned with the same $\varepsilon = 0.5$ and a few poses are assigned with $\varepsilon = 1$, which are the poses with high credibility. A suitable error metric called Root Mean Squared Error (RMSE) [22] is chosen to compute the optimization result against the ground truth solution.

Although the ground truth of the datasets is published, they and their corresponding ground truth contain different nodes for the different sampling frequency of front-end sensors. Therefore, [23] aligns them by searching for the best transformation to minimize the misalignment. This method called Absolute Trajectory Error (ATE) is included in the Rawseeds toolkit [19]. This tool is adopted in our evaluation to calculate the error between the optimized and the ground truth datasets. For the convenience of description we call all the resulting error RMSE. However this is essentially the ATE for the real-world datasets.

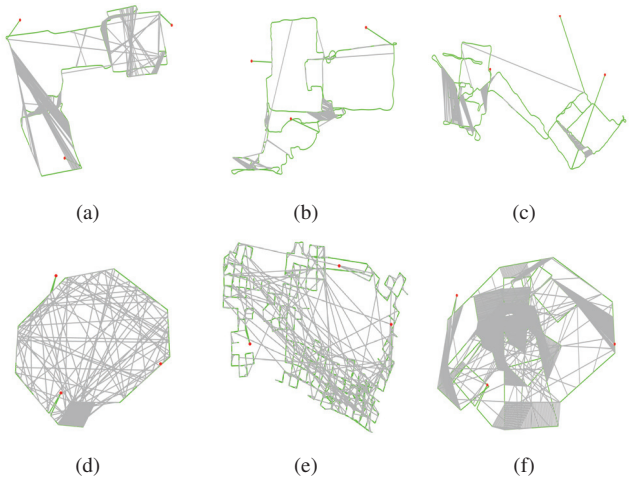

Fig. 3. Six of the datasets with added precise poses used in this comparison. From a to f: Bicocca, Bovisa04, Bovisa06, Ring, Manhattan, RingCity. The odometry is in green. The gray lines stand loop clousures. The red points are precise poses added manually.

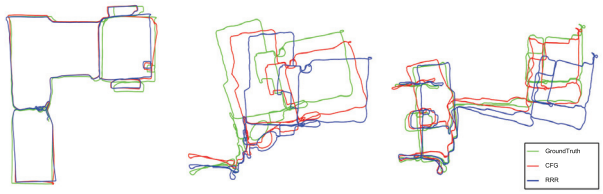

Fig. 4. The influence of different methods on three real datasets. Estimated trajectories for one of the Bicocca (a), Bovisa-04 (b), and Bovisa-06 (c) datasets. Colors distinguish the used method: CFG(red), RRR(blue), ground truth (green). Obviously, our method's results are closer to the ground truth than normal ones.

V. PROCESSING METHOD

A. Policies for comparing different methods

To prove the correctness and generality of our back-end optimizer, lots of contrast experiments are done among R-RR [21], Max-Mixtures [24], Novel [10] and proposed credibility factor graph(CFG). Since the parameters are changeful in different datasets, we assume that the free parameters of all algorithms can be referred from the known environment, or otherwise be fixed values for all the datasets.

For the Novel approach, the parameter which is the covariance of the switch node prior factor Ξ was assigned to 1 according to [10]. For the max-mixtures (MM) algorithm [24], mixture weight factor was set to 0.01 and the value of mixture scale factor was 10e-12, since they appeared to give the best results in common. For RRR [21], the odometry rate for real datas was set to 5, odometry rate for synthetic datasets equaled to 0 and place reconition rate was set to 1.

Three synthetic datasets and three real datasets with wrong loop closures are chosen. The wrong loop closures of three synthetic are made followed the rules in [10]. Three high-credibility poses which can form a big acute triangle are added to every datasets manually. For the sampling frequency of three real datasets are very fast, ten or more poses can be gotten in the same position during the data collection procedure. In order to improve the influence of the high-credibility poses, ten copies of every high-credibility poses are made to replace the ten consecutive poses in the datasets. Six changed datasets are showed in Fig. 3. Here we only need several high-credibility prior poses to increase the global accuracy largely. Our evaluation uses little high-credibility poses and five datasets to demonstrate the remarkable robustness of the system.

B. Policies for adding credibility factor

The high-credibility poses are introduced with three policies.

1) Random precise poses: This policy adds precise poses overall randomly. Most of the precise poses that are created using this policy will be dispersed and far away from each other.
2) Random angle precise poses: In real front-end, the place in the corner will be recognized more easily. Besides, the poses in the corner play a more important role in the optimization than the normal poses. Most of the angle precise poses are corners and chosen overall randomly.
3) Random group precise poses: Naturally, if one pose is characteristic, poses around it are more likely to be full of features. Therefore, these poses will be more precise than other poses given by the front-end sensor. This last policy updates the Random precise poses with another step by adding two precise poses beside the random precise poses to consist a local group.

Then the number proportion of added high-credibility poses was defined between 1/100 and 1/600, using the random precise poses policy. For each number of additional high-credibility poses, 20 trials were tested, with 100 tests per dataset in all.

C. Policies for mining least prior poses

To mine least prior poses, two kinds of policies are decided.

1) Least poses: One, two, three random prior poses are added to two datasets to test the effects of our optimizer. Every experiment repeats 20 times.
2) Best layout: Three prior poses are chosen by the constructed shapes which are divided into small acute triangle, big acute triangle and big obtuse triangle. Here, big triangle means the area of the triangle is larger than a quarter of the map area. For each shape of additional prior poses, 20 trials are tested, with 60 tests per dataset in all.

VI. RESULTS AND ANALYSIS

A. The results of different algorithms

Table I summarizes the accuracy of all the algorithm on different datasets in Fig. 3. In the last column the algorithm performed best with lowest mean trajectory error on every used dataset is marked in red "best". And the related

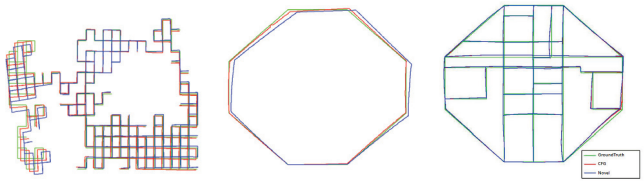

(a) (b) (c)

Fig. 5. The influence of different methods on three synthetic datasets. Estimated trajectories for one of the Manhattan (a), Ring (b), and RingCity (c) datasets. Colors distinguish the used methods: CFG(red), Novel (blue), ground truth (green).

TABLE I
THE RESULTS OF DIFFERENT METHODS ON FIVE DATASETS

Dataset	Novel	Max Mixtures	RRR	CFG	Best
Manhattan	1.18m	1.67m	11.64m	0.67m	CFG
Ring	4.39m	15.19m	5.29m	0.99m	CFG
RingCity	1.78m	41.21m	4.19m	1.08m	CFG
Bicocca	2.66m	3.94m	1.71m	1.32m	CFG
Bovisa-04	2.40m	11.89m	3.40m	1.99m	CFG
Bovisa-06	9.41m	7.90m	4.11m	1.24m	CFG

optimization results are presented in Fig. 4 and Fig. 5. Fig. 4 compares the estimated trajectories of three real datasets for CFG, RRR and ground truth, for RRR method makes a better performance on real datasets than MM and Novel. Obviously, the results using CFG method are more closer to ground truth. As Novel works well on three synthetic datasets, Fig. 5 gives a contrast among Novel, CFG and ground truth on synthetic datasets. We can see that the left part of mahatten datasets optimized by CFG is closer to ground truth than Novel. Besides, CFG approach also produced more accurate results than Novel on Ring and RingCity datasets.

From the Table I we can see, the CFG method works well in all of the datasets and can produce a more accurate result than other algorithm. Notice that the precision of Bovisa-06 datasets is little low by Novel, however, the result of CFG is improved largely .

The experimental results also show that our new optimizer can still remove those wrong loop closures and the low-credibility poses are dragged by those high-credibility poses at the same time. Remember that our marked matrix W only updates the Marquardt's Method [17]. As a result, those wrong loop closures can be removed by switch valuables easily using the first k_1 Guass-newton iterations. And according to the formulation of the proposed precise back-end in (11) and (14), the W which is given by front-end is used to keep those high-credibility poses fixed. Besides, step size h_M of Marquardt's Method which plays an important role in associating with all the poses will be recalculated at each iteration. Although those high-credibility poses are fixed after each iteration, they still influence other poses with the change of h_M. As a result, all the poses will approach the high-credibility poses slowly step by step. With our art precise and robust back-end, we achieve that remove those wrong loop closures and optimise the global pose graph with those fixed high-credibility poses.

B. The results of different pose adding policies

The results of different pose adding policies in mahatten datasets are shown in the Fig. 6(a). The first insight of Fig. 6(a) shows that the quality of the estimation by both Random angle precise poses policy and Random precise poses policy fluctuate a lot with variable precise poses. Next, it can be noticed that the Random group precise poses policy produces a low and stable result both in Fig. 6(a) and Fig. 6(b). Besides, The Random angle precise poses policy can get the lowest RMSEpos error. The RMSEpos of Novel method is 1.18 and CFG method with random group policy is 0.643. CFG method proposed in this paper reduced the error of 45%.

The Random precise poses policy is also used on C-ity10000 and Ring datasets in Fig. 6(c), which have similar rules with Fig. 6(a). Comparing to Table I, it can be found that the precision of maps is increased by all of the policies.

We have simulated almost all kinds of high-credibility poses and all the experiments show that our precise back-end can increase the accuracy of pose graph. Besides, we can find that stable result can be gotten by Random group precise poses policy for its inherent stability and a lowest error can be produced by Random angle precise poses policy. The reasons why best result can be gotten by Random angle precise poses policy are as follows: Firstly, front-end always collects more points for its special features that means the high-credibility poses in the corner can influence more points. Secondly, the data from front-end will be more prone to contain error for the orientation change of robot.

C. The results of mining policy

The results of our experiments with different datasets and CFG algorithms using mining policy are summarized in Table II that lists the mean trajectory errors. It can be seen that the results do not change a lot when only one or two random precise poses are added and good performance can be gotten when three random precise poses are added. However, the gap of Max error and Min error is a little large.

The most accurate map can be produced with least efficient prior poses when the prior poses can form a big acute triangle. Three poses can make good performance for the inherent stability of triangle. The reason why the big acute triangle poses can achieve best goal is that more poses can be affected by them for their uniform distribution in maps.

VII. CONCLUSION

This paper presents a novel approach to improve the accuracy and robustness of pose graph SLAM. The result shows that the CFG algorithm proposed in this paper can successfully increase the global accuracy to some extent. We have to point out that the prior points have to be collected in advance and the optimization time is little slow. We plan

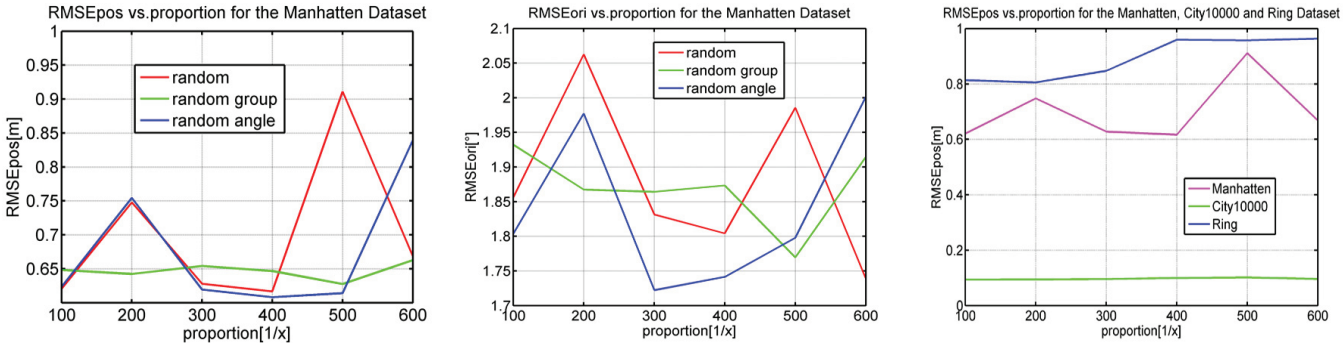

Fig. 6. The influence of the high-credibility poses on the accuracy of pose graph.

TABLE II

THE RESULTS OF MINING POLICY ON THREE DATASETS

Dataset	One Mean	Two Mean	Three Min	Three Mean	Three Max
Manhattan	1.10m	1.02m	0.61m	0.67m	1.05m
Ring	4.21m	4.15m	0.87m	0.99m	3.65m
Bicocca	2.65m	2.50m	1.24m	1.32m	2.01m

to enhance the automaticity and running speed of the CFG in our future research.

ACKNOWLEDGMENT

The work described in this paper is supported by National Natural Science Foundation of China (Grants No. 41401525), Natural Science Foundation of Guangdong Province (Grants No. 2014A030313209) and CRSRI Open Research Program (Program CKWV2014226/KY).

REFERENCES

[1] F. Lu and E. Milios, "Globally consistent range scan alignment for environment mapping," *Autonomous robots*, vol. 4, no. 4, pp. 333–349, 1997.

[2] E. Olson, J. Leonard, and S. Teller, "Fast iterative alignment of pose graphs with poor initial estimates," in *Robotics and Automation, 2006. ICRA 2006. Proceedings 2006 IEEE International Conference on*. IEEE, 2006, pp. 2262–2269.

[3] U. Frese and L. Schroder, "Closing a million-landmarks loop," in *Intelligent Robots and Systems, 2006 IEEE/RSJ International Conference on*. IEEE, 2006, pp. 5032–5039.

[4] M. Kaess, A. Ranganathan, and F. Dellaert, "isam: Incremental smoothing and mapping," *Robotics, IEEE Transactions on*, vol. 24, no. 6, pp. 1365–1378, 2008.

[5] M. Kaess, H. Johannsson, R. Roberts, V. Ila, J. Leonard, and F. Dellaert, "isam2: Incremental smoothing and mapping with fluid relinearization and incremental variable reordering," in *Robotics and Automation (ICRA), 2011 IEEE International Conference on*. IEEE, 2011, pp. 3281–3288.

[6] R. Kummerle, G. Grisetti, H. Strasdat, K. Konolige, and W. Burgard, "g 2 o: A general framework for graph optimization," in *Robotics and Automation (ICRA), 2011 IEEE International Conference on*. IEEE, 2011, pp. 3607–3613.

[7] G. H. Lee, F. Fraundorfer, and M. Pollefeys, "Robust pose-graph loop-closures with expectation-maximization," in *Intelligent Robots and Systems (IROS), 2013 IEEE/RSJ International Conference on*, 2013, pp. 556–563.

[8] L. Carlone, A. Censi, and F. Dellaert, "Selecting good measurements via l relaxation: A convex approach for robust estimation over graphs," in *Intelligent Robots and Systems (IROS 2014), 2014 IEEE/RSJ International Conference on*, 2014, pp. 2667 – 2674.

[9] N. Sunderhauf and P. Protzel, "Towards a robust back-end for pose graph slam," in *Robotics and Automation (ICRA), 2012 IEEE International Conference on*. IEEE, 2012, pp. 1254–1261.

[10] ——, "Switchable constraints for robust pose graph slam," in *Intelligent Robots and Systems (IROS), 2012 IEEE/RSJ International Conference on*. IEEE, 2012, pp. 1879–1884.

[11] S. Schwertfeger, A. Jacoff, C. Scrapper, J. Pellenz, and A. Kleiner, "Evaluation of maps using fixed shapes: the fiducial map metric," in *Proceedings of the 10th Performance Metrics for Intelligent Systems Workshop*. ACM, 2010, pp. 339–346.

[12] C. Satirapod and P. Homniam, "Gps precise point positioning software for ground control point establishment in remote sensing applications," *Journal of surveying engineering*, vol. 132, no. 1, pp. 11–14, 2006.

[13] T. Korah and C. Rasmussen, "Probabilistic contour extraction with model-switching for vehicle localization," in *Intelligent Vehicles Symposium, 2004 IEEE*. IEEE, 2004, pp. 710–715.

[14] M. Montemerlo and S. Thrun, "Large-scale robotic 3-d mapping of urban structures," in *Experimental Robotics IX*. Springer, 2006, pp. 141–150.

[15] R. Kümmerle, B. Steder, C. Dornhege, A. Kleiner, G. Grisetti, and W. Burgard, "Large scale graph-based slam using aerial images as prior information," *Autonomous Robots*, vol. 30, no. 1, pp. 25–39, 2011.

[16] N. Suenderhauf, "Robust optimization for simultaneous localization and mapping," *PhD Thesis, Chemnitz University of Technology*, 2012.

[17] C. Hertzberg, "A framework for sparse, non-linear least squares problems on manifolds," in *UNIVERSITÄT BREMEN*. Citeseer, 2008.

[18] F. R. Kschischang, B. J. Frey, and H.-A. Loeliger, "Factor graphs and the sum-product algorithm," *Information Theory, IEEE Transactions on*, vol. 47, no. 2, pp. 498–519, 2001.

[19] S. Ceriani, G. Fontana, A. Giusti, D. Marzorati, M. Matteucci, D. Migliore, D. Rizzi, D. G. Sorrenti, and P. Taddei, "Rawseeds ground truth collection systems for indoor self-localization and mapping," *Autonomous Robots*, vol. 27, no. 4, pp. 353–371, 2009.

[20] Vertigo, "Versatile extensions for robust inference using graph optimization," http://www.openslam.org/vertigo.

[21] Y. Latif, C. Cadena, and J. Neira, "Robust loop closing over time." MIT Press, 2013, p. 233.

[22] R. Kümmerle, B. Steder, and C. Dornhege, et al., "On measuring the accuracy of slam algorithms," *Autonomous Robots*, vol. 27, no. 4, pp. 387–407, 2009.

[23] N. Sunderhauf and P. Protzel, "Switchable constraints vs. max-mixture models vs. rrr-a comparison of three approaches to robust pose graph slam," in *Robotics and Automation (ICRA), 2013 IEEE International Conference on*. IEEE, 2013, pp. 5198–5203.

[24] E. Olson and P. Agarwal, "Inference on networks of mixtures for robust robot mapping," *The International Journal of Robotics Research*, vol. 32, no. 7, pp. 826–840, 2013.